

## Resonant and nonresonant behavior of the heavy-ion reaction $^{14}\text{C} + ^{12}\text{C}$

R. M. Freeman, Z. Basrak,\* F. Haas, A. Hachem,<sup>†</sup> G. A. Monnehan,<sup>‡</sup> and M. Youlal  
*Centre de Recherches Nucléaires, Institut National de Physique Nucléaire et de Physique des Particules—Centre National de la Recherche Scientifique/Université Louis Pasteur, B.P. 20, F-67037 Strasbourg CEDEX, France*

(Received 9 March 1992)

The  $^{14}\text{C} + ^{12}\text{C}$  reaction has been studied by a kinematic coincidence technique at 13 incident energies ranging from  $E_{\text{c.m.}} = 19.35$  to 24.9 MeV. The resonances previously reported from  $\gamma$ -ray yield measurements were observed in the equivalent excitation functions, as well as in the large angle elastic scattering data, of the present measurements. Spin assignments were made to the two resonances in this energy range. These resonances are members of a band with angular momenta several units larger than the grazing values corresponding to  $^{14}\text{C}$  and  $^{12}\text{C}$  orbiting about each other at a distance significantly outside the strong absorption radius. Other structures which were observed were unrelated to the resonant behavior.

PACS number(s): 25.70.Bc, 25.70.Ef

### I. INTRODUCTION

The excitation functions of the  $^{14}\text{C} + ^{12}\text{C}$  reaction show a series of resonantlike structures which were first observed in  $\gamma$ -ray intensity measurements [1]. Although the origin of these resonances was unknown it was assumed that they arose from some mechanism involving the grazing partial waves. This assumption was supported by the calculations of Haas and Abe [2] who found that the number of open channels available to the grazing partial waves of the  $^{14}\text{C} + ^{12}\text{C}$  system dipped to relatively low values when their angular momenta  $L_g$  lay in the range of about 15–20 units, i.e., at about  $E_{\text{c.m.}} = 25$  MeV. The weaker absorption implied by the smaller number of open channels could allow resonant effects to show up within an energy window which agrees roughly with the region where structures were observed. A possible mechanism with attendant spin assignments of  $J = 15$ , 16, and 17 for the resonances at energies around  $E_{\text{c.m.}} = 21$ , 23.5, and 25.5 MeV, respectively, was proposed by Tanimura [3].

More recently Konnerth *et al.* [4] have studied the  $^{14}\text{C} + ^{14}\text{C}$  reaction and concurrently channels of the  $^{14}\text{C} + ^{12}\text{C}$  reaction as a consequence of the important fraction of  $^{12}\text{C}$  in their target. They found that the  $L = 18$  partial wave resonates at the structure peaking at  $E_{\text{c.m.}} = 23.5$  MeV. As the grazing angular momentum  $L_g$  at this energy is only 15 (a spin assignment  $J = 16$  was proposed by Tanimura) it is clear that the explanation for these resonances must require a mechanism where the nuclei interact at larger separation distances than had

hitherto been supposed. Similar conclusions had been reached in the case of the resonant behavior of the  $^{14}\text{C} + ^{16}\text{O}$  reaction [5]. We have therefore undertaken particle measurements to verify whether the spins of the resonances of  $^{14}\text{C} + ^{12}\text{C}$  are as high as claimed using a technique similar to that of Konnerth *et al.*, and identical to that which we employed for the  $^{14}\text{C} + ^{16}\text{O}$  system. The bombarding energies were chosen to encompass two of the most prominent resonances which appeared in the  $\gamma$ -ray work. As we will report in Sec. III we have confirmed the findings of Konnerth *et al.* that the resonating partial waves have significantly higher angular momenta than grazing partial waves. The results also vindicate their proposed description of the resonances in terms of a molecular configuration where the exchange of the outermost nucleons provides the binding between the nuclear cores. Although qualified as highly speculative at the time this description is quite in keeping with the picture which emerges from the present data.

### II. EXPERIMENT

The  $^{14}\text{C} + ^{12}\text{C}$  reaction was studied using the radioactive  $^{14}\text{C}$  beam from the Strasbourg MP tandem Van de Graaff. These measurements were made during the same series as the  $^{14}\text{C} + ^{16}\text{O}$  experiment [5] with the same experimental geometry. The target was a self-supporting carbon foil nominally  $20 \mu\text{g}/\text{cm}^2$  thick. To cover the energy region where two of the resonances of our earlier  $\gamma$ -ray data at  $E_{\text{c.m.}} = 20.75$  and 23.5 MeV were observed, runs were made at 13 bombarding energies ranging from  $E_{\text{lab}} = 41.92$ –53.95 MeV. Repeat runs were made at the end of the experiment to estimate the carbon buildup on the target. During the measurements one run was made with a 50-MeV  $^{12}\text{C}$  beam as a check on our absolute cross sections and angular distributions [6,7]. Where possible our cross sections were verified against previous data [4,8] and the agreement is acceptable considering the 20% error assigned to the present absolute values.

As described in our  $^{14}\text{C} + ^{16}\text{O}$  article a standard kine-

\*Permanent address: Ruder Boskovic Institute, Zagreb, Croatia.

<sup>†</sup>Permanent address: Département de Physique, Université de Nice Sophia-Antipolis, France.

<sup>‡</sup>Present address: Université Nationale FAST—Département de Physique, Abidjan, Ivory Coast.

matic coincidence setup was used to measure the angular distributions of the outgoing channels as a function of bombarding energy. The outgoing particles were detected in coincidence in two position-sensitive silicon detectors, one placed to cover the laboratory angles  $22^\circ$  to  $50^\circ$  and the other detector  $-42^\circ$  to  $-70^\circ$ . A spectrum of the masses detected in the more forward detector, deduced from the kinematic relation between the two coincident particles, is displayed in Fig. 1. For masses  $\leq 10$  the limiting angle of the associated particle is less than the minimum angle of the second detector and consequently only one coincidence branch (heavier partner in the most forward detector, lighter in the second) can appear. It is noteworthy that in this figure the dominant binary channels of the reaction are for masses 12–14, i.e.,  $^{12}\text{C}$ ,  $^{13}\text{C}$ , and  $^{14}\text{C}$ . The  $^{16}\text{O} + ^{10}\text{Be}$  channel, for example, is surprisingly weak compared with channels involving the rearrangement of neutrons.

Selecting the  $M = 13$  peak and angles compatible with the  $^{13}\text{C} + ^{13}\text{C}^*$  channel kinematics  $Q$ -value spectra have been constructed from the parameters of the coincident events and are shown in Fig. 2 for all 13 incident energies. The most intense peak is the unresolved doublet of  $^{13}\text{C}$  at 3.68–3.85 MeV where two resonances are clearly visible. These two resonances are consistent with the structures observed earlier in our  $\gamma$ -ray data for the yield functions of transitions from the 3.85-MeV level of  $^{13}\text{C}$ . On the other hand, the channel to the ground states of  $^{13}\text{C}$  appears to fluctuate in a manner little correlated with the resonances. The results selecting mass 17, i.e., channel  $^{17}\text{O} + ^9\text{Be}$ , are shown in Fig. 3.  $^9\text{Be}$  has no bound excited states so only peaks corresponding to the four bound states of  $^{17}\text{O}$  are seen. Very strong fluctuations in the ground-state cross section are evident.

Angular distributions were determined for some of the outgoing channels. These were integrated over wide angular ranges to approximate to a yield function for the channel. In the case of weak channels the intensities of the excitation functions were obtained simply by summing the number of counts and are expressed in arbitrary units. The  $^{13}\text{C} + ^{13}\text{C}$  channel is special in that no distinction can be made between the two identical nuclei. Hence our cross sections for this channel are larger by an

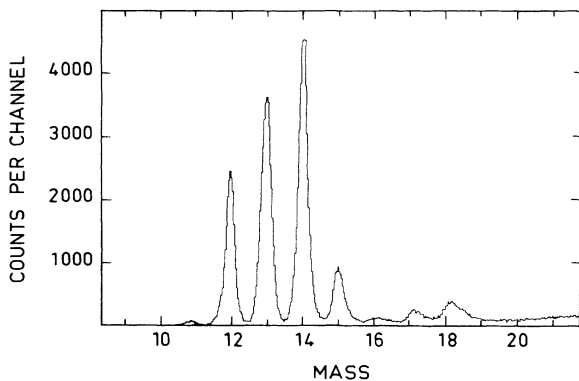


FIG. 1. Typical mass spectrum constructed from the information in the coincident events.

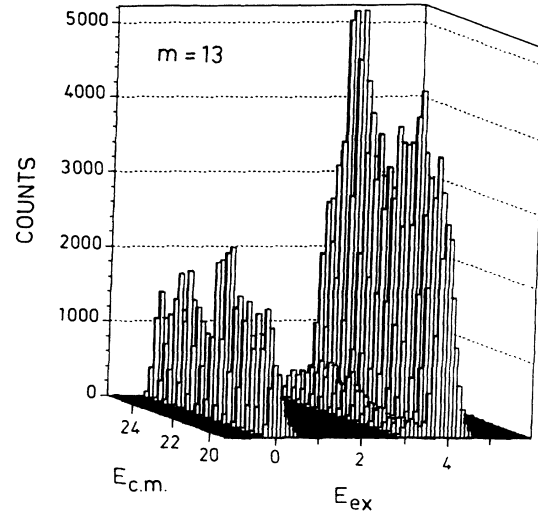


FIG. 2. Variation of the  $^{13}\text{C} + ^{13}\text{C}$  channels with bombarding energy. The resonant structure is visible in the peak of the unresolved 3.68–3.85-MeV doublet.

extra factor of 2 which has to be taken into account when comparing with the inverse reaction data of Korotky *et al.* [8]. In principle different excited states of  $^{13}\text{C}$  can be distinguished but this is not feasible in practice and our cross sections for the  $^{13}\text{C} + ^{13}\text{C}^*$  channels are therefore the sum of intensities at angles  $\theta$  and  $180^\circ - \theta$ .

Although the kinematic coincident technique is designed to study the binary channels results were also obtained for the  $^{12}\text{C}(^{14}\text{C}, 2\alpha)^{18}\text{O}$  reaction. Where only two of the three outgoing particles are detected there is sufficient information to reconstruct the kinematics provided the masses of the detected particles are known. In the present experimental setup these masses are not

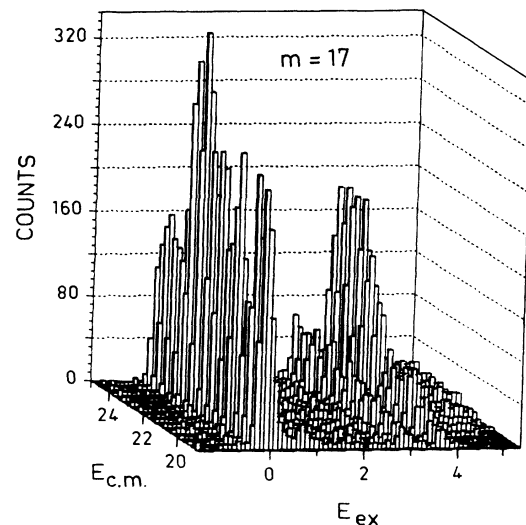


FIG. 3. Variation of the  $^{17}\text{O} + ^9\text{Be}$  channels with bombarding energy. Note the strong fluctuations for the ground-state peak.

known for events more complex than binary. However it was found that a large portion of these events were due to coincidences between the two  $\alpha$  particles of the  $2\alpha + {}^{18}\text{O}$  channel. Thus by suppressing binary events (total mass of 26) and assuming that the remainder were  $\alpha$ - $\alpha$  coincidences a relatively clean spectrum of  ${}^{18}\text{O}$  states could be obtained. The results of this analysis will be presented in Sec. IV.

### III. RESULTS FOR THE C+C CHANNELS

The results for channels which are observed to resonate are assembled in Fig. 4 with earlier  $\gamma$ -ray work to show the concordance which exists between the two techniques (the  $\gamma$ -ray measurements reproduced here were recorded in parallel with  ${}^{14}\text{C} + {}^{14}\text{C}$  data taken at Munich [9] and have been partially published elsewhere [10]). The two techniques do not measure precisely the same cross sections though, as Fig. 4 indicates, the resonant component is common to both. From the combined results of both techniques in Figs. 4(a)–4(d) we learn that there is resonant structure in the simple excitation of the 3.85-MeV level of  ${}^{13}\text{C}$  and the 6.73-MeV level of  ${}^{14}\text{C}$ . In Fig. 4(e) the results for another channel which has been observed to resonate are included. This is the cross section for large angle elastic scattering which can be interpreted as arising from the exchange of a pair of neutrons

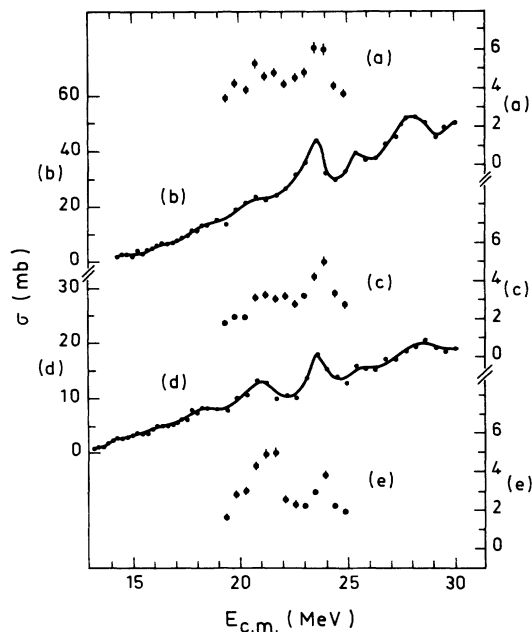


FIG. 4. Comparison between excitation functions of previous  $\gamma$ -ray measurements (b) and (d) and the present results: (a)  ${}^{13}\text{C}_{g.s.} + {}^{13}\text{C}^*$  for the unresolved 3.68–3.85-MeV doublet ( $50^\circ$ – $75^\circ$ ), (b) feeding of the 3.85-MeV level of  ${}^{13}\text{C}$  from the  $\gamma$ -ray intensity measurements, (c)  ${}^{14}\text{C}^* + {}^{12}\text{C}_{g.s.}$  for the unresolved group of states including the 6.73-MeV level of  ${}^{14}\text{C}$  ( $55^\circ$ – $85^\circ$ ), (d) feeding of the 6.73-MeV level of  ${}^{14}\text{C}$  from the  $\gamma$ -ray intensity measurements, and (e) elastic channel at large angles ( $95^\circ$ – $135^\circ$ ). The degrees in brackets are the ranges over which the angular distributions were integrated.

between the two  ${}^{12}\text{C}$  cores.

Elastic angular distributions are shown in Fig. 5 for all 13 incident energies. Almost pure  $L = 16$  and 18 forms are observed for the lower and upper resonances, respectively, in the region of large angle elastic scattering where the transfer elastic component, arising from the neutron exchange, dominates. The elastic angular distributions on-resonance, as well as at an intermediate energy, are shown in Fig. 6 where they are compared with  $P_L^2(\cos\theta)$  shapes. The  $L = 18$  assignment to the upper resonance was already made by Konnerth *et al.* and the present results are in complete agreement. A regular series of small structures is observed in the  $\gamma$ -ray yield functions to precede these two resonances at approximately  $E_{c.m.} = 14, 16, \text{ and } 18$  MeV. They are shown on a more expanded scale in Fig. 7 for the inelastic channel where they have been tentatively identified as the  $J^\pi = 10^+, 12^+, \text{ and } 14^+$  members, respectively, of the same band of resonances. As illustrated in Fig. 7 the five resonances fall on a line given by the expression

$$E_{c.m.} = \alpha L(L+1) + E_0, \quad (1)$$

where the rotational parameter ( $\alpha = \hbar^2/2I$ ) is found to be

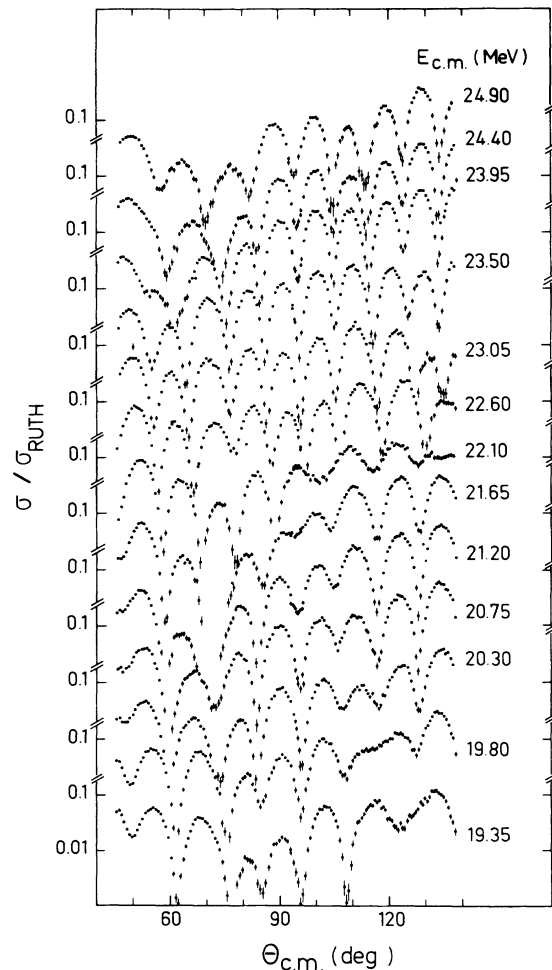


FIG. 5. Elastic angular distributions of the  ${}^{14}\text{C} + {}^{12}\text{C}$  reaction for all energies studied.

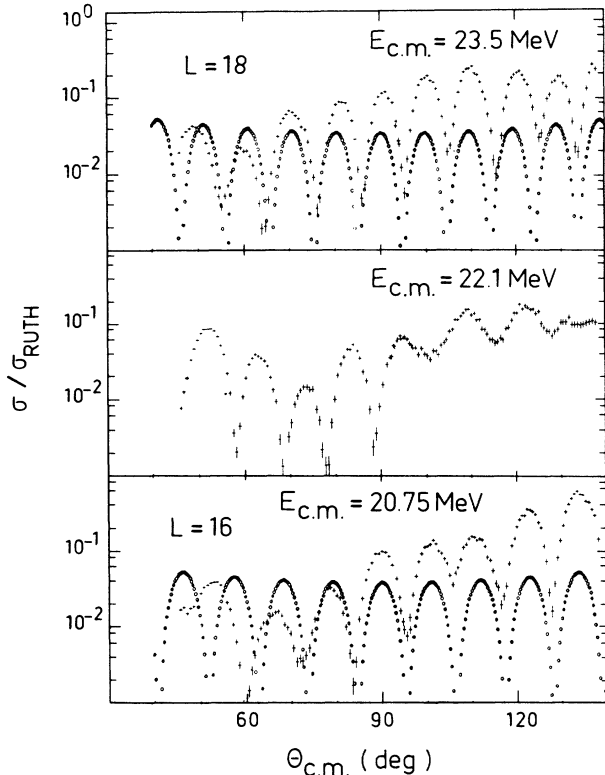


FIG. 6. Elastic angular distributions of the  $^{14}\text{C} + ^{12}\text{C}$  reaction at the two resonances and at an intermediate energy. Comparison is made with the  $P_L^2(\cos\theta)$  forms for  $L = 16$  and  $18$ .

40 keV ( $I = 5.4 \times 10^{-42} \text{ MeV s}^2$ ) and the bandhead  $E_0$  is 9.8 MeV ( $E_{\text{ex}}[^{26}\text{Mg}] = 29.0 \text{ MeV}$ ). The moment of inertia  $I$  is given by the expression

$$I = \frac{2}{5} (A_1 r_1^2 + A_2 r_2^2) + \mu R^2, \quad (2)$$

where  $\mu$  is the reduced mass and  $R$  the distance between

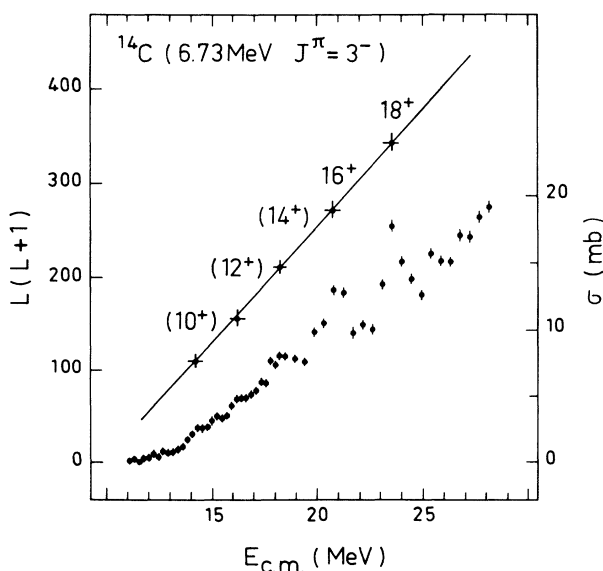


FIG. 7.  $\gamma$ -ray intensity measurements for the 6.73-MeV level of  $^{14}\text{C}$  [see Fig. 4(d)] showing the proposed high moment of inertia band.

the two nuclear centers. The nuclear radii of  $^{14}\text{C}$  and  $^{12}\text{C}$ ,  $r_1$ , and  $r_2$  (mass radii taken equivalent to the charge radii), are calculated with a radius parameter of 1.2 fm. From the experimental moment of inertia we are thus led to a two-center distance  $R$  which corresponds to the two carbon nuclei orbiting around each other at a distance of 8.2 fm, well outside the strong interaction radius of 6.9 fm given by the expression

$$1.36(A_1^{1/3} + A_2^{1/3}) + 0.5. \quad (3)$$

The moment of inertia as expressed by Eq. (2) implies a rigid rotation of the system (the sticking limit) as often assumed for closer nuclear collisions where there is appreciable friction between the interacting ions. In the present case of a more distant collision this approximation may no longer be adequate. As a consequence, the interaction radius deduced from the moment of inertia may be even larger since with reduced friction only the term  $\mu R^2$  will tend to remain in Eq. (2) yielding in the limit  $R = 9.0 \text{ fm}$ .

The energy of the bandhead should be roughly equal to the Coulomb barrier  $E_0 \approx E_{\text{CB}}$ . But at a distance of 8.2 fm the inter-ion Coulomb potential is only 6.3 MeV compared with the value 9.8 MeV found for  $E_0$ . The moment of inertia found experimentally also falls outside the systematics compiled for resonances in other heavy-ion systems [11,12]. Using the expression for the moment of inertia given in these references, which differs only in detail from Eq. (2) above (in particular their model is based on a grazing encounter  $R = r_1 + r_2$ ), then  $I$  is calculated to be  $3.54 \times 10^{-42} \text{ MeV s}^2$  whereas the experimental value is more than 50% greater. In spite of the large distance between the two nuclear centers which follows from our estimated moment of inertia, of the 160-mb of flux in the incoming  $L = 18$  partial wave at resonance, more than 20 mb exit in identified resonating reaction channels and a comparable fraction returns to the elastic via the transfer of a neutron pair. Nothing more than the rearrangement of neutrons is required in the resonant processes.

The assumptions of the foregoing discussion concerning how the resonances are assembled into a band were made in order to obtain a more quantitative determination of the rotational parameter and subsequently the two-center distance between the orbiting nuclei. Even without those assignments which remain to be tested it is nevertheless evident that this distance is larger than the strong interaction radius of Eq. (3) as illustrated in Fig. 8 where the  $90^\circ$  elastic scattering results of the present work are compared to the gross structure occurring in  $^{14}\text{C} + ^{14}\text{C}$  [13] and  $^{12}\text{C} + ^{12}\text{C}$  (reproduced in Ref. 8). The energy scale is appropriate for  $^{14}\text{C} + ^{12}\text{C}$  but to take account of the increasing size of the nuclei with mass it has been modified for the other two reactions to line up their grazing angular momenta. Leaving aside certain differences between the  $^{14}\text{C} + ^{14}\text{C}$  and  $^{12}\text{C} + ^{12}\text{C}$  reactions, notably the intermediate structure which has been smoothed out of the  $^{12}\text{C} + ^{12}\text{C}$  results, the gross structure in both cases is similar arising essentially from peripheral effects which can be simulated using surface-transparent optical model potentials. The partial waves responsible for the structures have angular momenta close to the

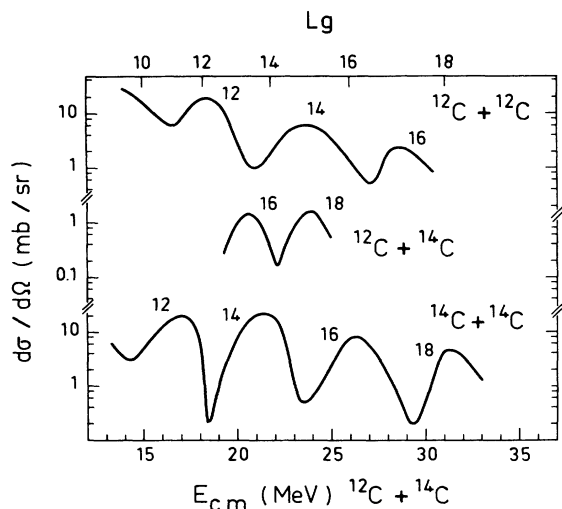


FIG. 8. The  $90^\circ$  elastic data showing the gross structure of the  $^{12}\text{C}+^{12}\text{C}$  and  $^{14}\text{C}+^{14}\text{C}$  reactions compared with the present measurements for the  $^{14}\text{C}+^{12}\text{C}$  system. Note that the energy scale applies to  $^{14}\text{C}+^{12}\text{C}$  and has been modified for the other two systems in order that the grazing angular momenta correspond.

grazing values contrasting with the situation for  $^{14}\text{C}+^{12}\text{C}$  where the angular momenta are about 3 units greater. The features distinguishing the  $^{14}\text{C}+^{12}\text{C}$  system from the other two systems can be understood qualitatively by considering the channels available for the exchange of nucleons. As remarked with respect to Fig. 1 most of the outgoing flux from the  $^{14}\text{C}+^{12}\text{C}$  reaction is in the rearrangement of the neutrons. The  $Q$  value for a one-neutron transfer reaction is  $-3.2$  MeV and for the transfer of two neutrons from  $^{14}\text{C}$  to  $^{12}\text{C}$  it is trivially zero. For the  $^{12}\text{C}+^{12}\text{C}$  system the rearrangement of one or two neutrons (or protons) requires at minimum nearly 14 MeV and for  $^{14}\text{C}+^{14}\text{C}$  nearly 7 MeV. These very negative  $Q$  values will result in unfavorable matching conditions for nucleon exchange in the two identical boson systems.

The properties of the resonant behavior of this reaction, i.e., the channels which resonate involve the rearrangement of neutrons at a distance where only the tail of the nuclear densities interact, strongly suggest that the resonances are due to molecular configurations that are held together by the sharing of valence neutrons. The symmetry of the system composed of two  $^{12}\text{C}$  cores bound by a pair of neutrons would also explain the absence of the odd  $L$  members of the band. Such a system with isospin  $T=1$  and spin  $S=0$  has been discussed by von Oertzen and Bohlen [14]. The molecular states are split according to whether they are excited by even or odd  $L$  partial waves ( $L=J$ , the spin of the molecular state in this case). Presumably it is the lowest energy molecular band of even  $J$  states which appears in the present data.

Excitation functions for other C+C channels are shown in Fig. 9. Apart from the large angle data for the

excitation of the 6.73-MeV state of  $^{14}\text{C}$ , where resonant behavior could be anticipated, the situation in other channels is less clear for though structures are observed the correlation with the resonances is not too evident. In particular for the  $^{13}\text{C}+^{13}\text{C}$  outgoing channel, for which calculations based on molecular orbits exist [8,15,16], correlation with the resonant structure is only minor if present at all. Since the spin of  $^{13}\text{C}$  is  $\frac{1}{2}$  the angular momenta  $L$  in the entrance and exit channels are identical and indications of this  $L$  may be found in the angular distributions. An example of an angular distribution at the energy of the upper resonance is shown in Fig. 10. It fits more closely to an  $L=16$  rather than to the  $L=18$  form assigned to the resonance which is further evidence that the channel participates little in the resonant mechanism. Konnerth *et al.* [4] remarked on the comparative weakness of the inelastic channel to the  $2^+$  (4.44 MeV) state of  $^{12}\text{C}$ . Over the larger angular range of the present data the dominance of the strength of the inelastic channels to

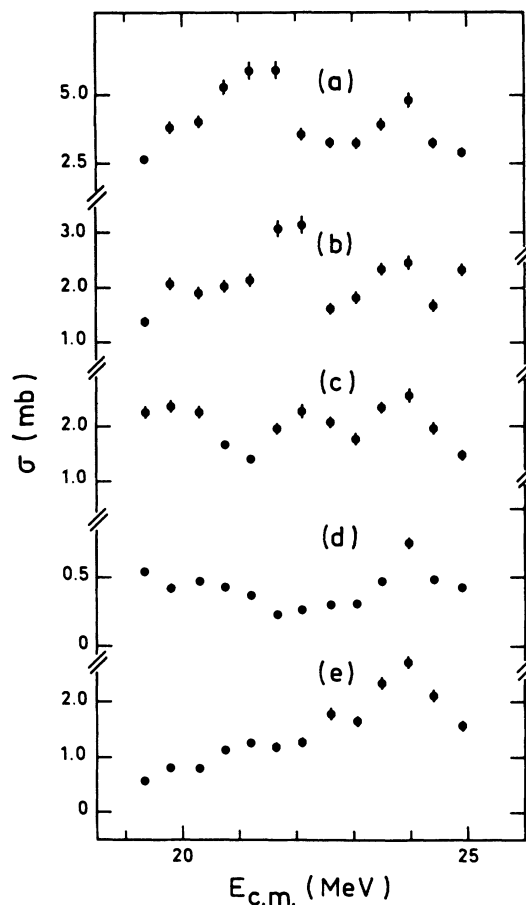


FIG. 9. Excitation functions for other C+C channels compared with the resonant structure (a) of the large angle elastic scattering: (a) elastic channel at large angles ( $95^\circ-135^\circ$ ), (b)  $^{13}\text{C}_{g.s.}+^{13}\text{C}_{g.s.}$  ( $50^\circ-85^\circ$ ), (c)  $^{14}\text{C}_{g.s.}+^{12}\text{C}^*$  for the 4.44-MeV level of  $^{12}\text{C}$  ( $50^\circ-85^\circ$ ), (d) as for (c) but at larger angles ( $105^\circ-130^\circ$ ), (e)  $^{14}\text{C}^*+^{12}\text{C}_{g.s.}$  at large angles for the unresolved group of states including the 6.73-MeV level of  $^{14}\text{C}$  ( $115^\circ-132^\circ$ ). The degrees in parentheses are the ranges over which the angular distributions were integrated.

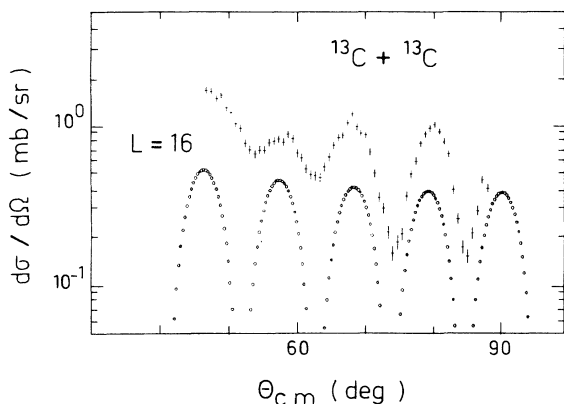


FIG. 10. Angular distribution of the  $^{13}\text{C}_{g.s.} + ^{13}\text{C}_{g.s.}$  channel at  $E_{c.m.} = 23.5$  MeV.

the  $3^-$  state of  $^{14}\text{C}$  relative to the  $2^+$  state of  $^{12}\text{C}$  is not so apparent.

The particular features which characterize the two channels which do resonate will now be considered. These channels, i.e., the excitation of the 6.73-MeV state of  $^{14}\text{C}$  and the 3.85-MeV state of  $^{13}\text{C}$ , both have a  $Q$  value of about  $-7$  MeV and decrease by 3 units of angular momenta in the outgoing channels. The dynamics are very similar because the two channels are closely related by their nuclear structure; a more explicit description will shortly follow. For grazing collisions there is good matching between the entrance and exit channels in both reactions as pointed out in our first article [1]. However the grazing assumption is now superseded by our estimated energy versus  $L$  dependence for the resonances, i.e.,  $0.040L(L+1)$  MeV where a change of 3 units of  $L$  is equivalent to an energy change of only about 4 MeV. Thus the matching is not as favorable as formerly supposed and not the overriding factor. The prime reason should be sought in the affinity between the molecular configuration and the outgoing channels. Intuitively, the resonant excitation of the 6.73-MeV level of  $^{14}\text{C}$  could be expected. The formation of a pear-shaped octupole state is the type of deformation which might result from the breakup of a configuration consisting of two  $^{12}\text{C}$  cores bridged by the pair of valence neutrons. When viewed from the shell model the relation with the other resonating channel becomes apparent. The dominant configuration of the two valence neutrons of the 6.73-MeV ( $J^\pi = 3^-$ ) state of  $^{14}\text{C}$  is  $d_{5/2}p_{1/2}$  [17]. Knowing that the valence neutron of the 3.85-MeV state of  $^{13}\text{C}$  is in the  $d_{5/2}$  subshell it follows that the two channels can be interchanged simply by displacing either one of the valence neutrons, without changing its quantum numbers, from one  $^{12}\text{C}$  core to the other. Under this symmetric exchange of a single neutron one channel can be transformed into the other.

Another reaction which exhibits similar features is  $^{14}\text{C} + ^{16}\text{O}$  [5]. Considering the role of nucleon exchange in these reactions it is probably significant that, in common with the  $^{14}\text{C} + ^{12}\text{C}$  reaction, the target and projectile nuclei differ by a pair of nucleons. In both reactions the large angle elastic scattering is correlated with resonances

in reaction channels. If the  $^{14}\text{C} + ^{12}\text{C}$  system has given the clearest indications of the formation of a molecular configuration this can be ascribed to its greater simplicity since only two valence neutrons are principally involved in the exchange processes.

#### IV. OTHER CHANNELS

Other binary channels are weak as can be judged from Fig. 1. These channels require a fairly complex rearrangement of the nucleons and are unlikely to be strongly coupled to any simple mode associated with the resonant effects. Although nothing correlated with the resonances was observed various structures appear in the energy dependence and a selection is displayed in Fig. 11. In particular the strong fluctuations of the  $^{17}\text{O} + ^9\text{Be}$  channel, also visible in Fig. 3, are included. Structures of this type have been seen in other reactions (see, for example, the  $^{12}\text{C} + ^{24}\text{Mg}$  data of Glaesner *et al.* [18]) and have been interpreted as Ericson fluctuations in a dinuclear system. They also coexist in the C+C channels (see Fig. 4) with the resonant structure. The inclusive  $\gamma$ -ray technique tends to wash out such fluctuations to a level where they are difficult to detect.

The yield function for the 1.27-MeV  $\gamma$ -ray transition of  $^{12}\text{Ne}$  is reproduced from Ref. [10] in Fig. 12. This transi-

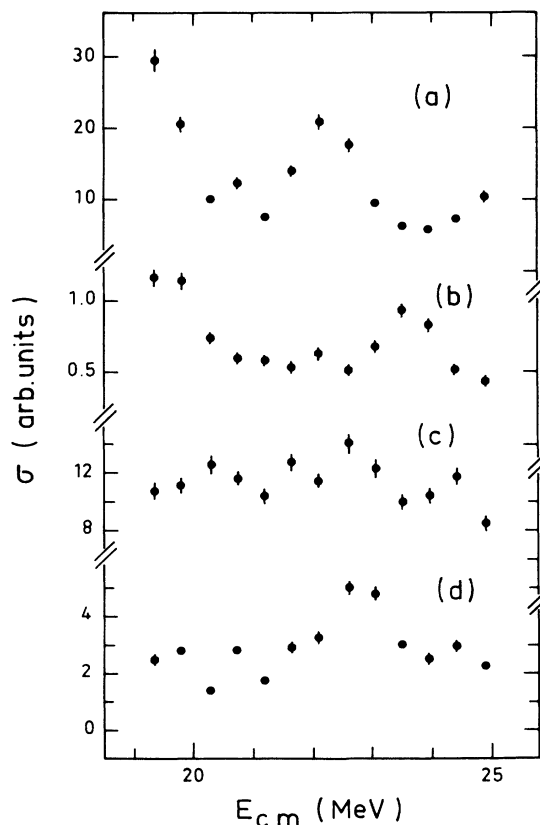


FIG. 11. Excitation functions for some weak channels obtained by summing the coincident counts: (a)  $^{18}\text{O}^* + ^8\text{Be}_{g.s.}$  for the 1.98-MeV level of  $^{18}\text{O}$ , (b)  $^{16}\text{O}_{g.s.} + ^{10}\text{Be}_{g.s.}$ , (c)  $^{15}\text{N}_{g.s.} + ^{11}\text{B}_{g.s.}$ , (d)  $^{17}\text{O}_{g.s.} + ^9\text{Be}_{g.s.}$ .

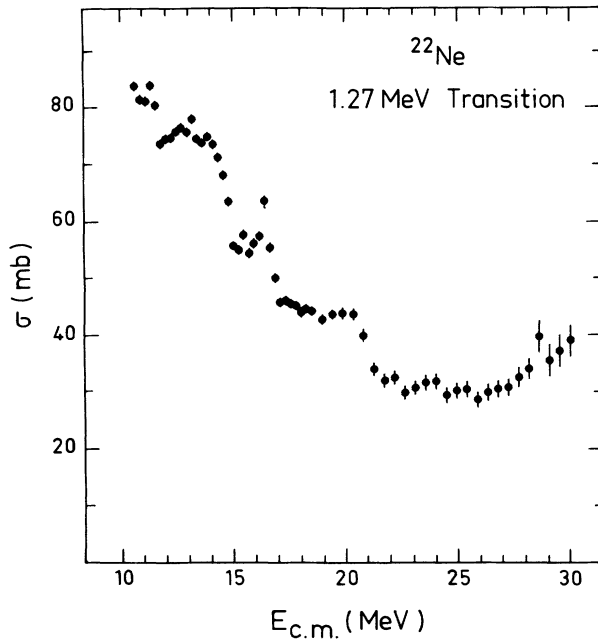


FIG. 12. Yield function of the 1.27-MeV  $\gamma$ -ray transition of  $^{22}\text{Ne}$ .

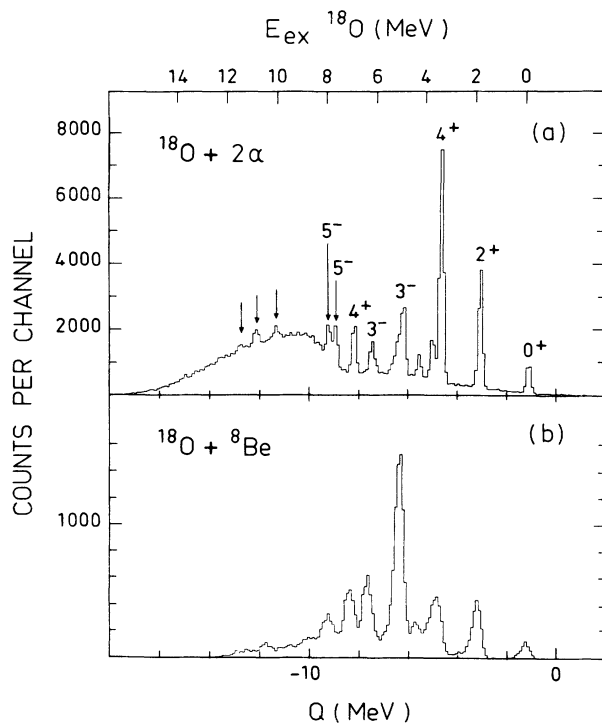


FIG. 13. Spectra of states of  $^{18}\text{O}$  excited by (a) the  $^{14}\text{C}(^{12}\text{C}, 2\alpha)$  and (b) the  $^{14}\text{C}(^{12}\text{C}, ^8\text{Be})$  reaction which have been reconstructed from the coincident events as explained in the text. In both cases the spectra are the sum of results for the 7 highest incident energies. Three high spin states appearing in the continuum in (a) are indicated by arrows.

tion generally follows the emission of a single  $\alpha$  particle though the rise at higher energies shows that other channels like  $2p2n$  are beginning to contribute. Little remains of the strong structure apparent at lower energies in the higher energy region where the present measurements were made. In this region most of the cross section for the emission of  $\alpha$  particles is in the  $2\alpha$  and  $\alpha n$  channels. As explained in Sec. II the  $2\alpha$  channel feeding states of  $^{18}\text{O}$  is responsible for much of the background in the coincidence spectra. In fact the states of  $^{18}\text{O}$  can be reached in two ways via the coincidences: (1)  $\alpha$  particles from the fusion-evaporation process are detected in coincidence and the total kinetic energy corrected for the missing recoil energy of  $^{18}\text{O}$  or (2) from the breakup of the ground state of  $^8\text{Be}$  where the two  $\alpha$  particles stay so close together that they are often detected as a single mass 8 particle in coincidence with  $^{18}\text{O}$  and can be treated like other binary channels. Spectra for the excitation of  $^{18}\text{O}$  can be reconstructed from the coincident events for both situations and are shown in Fig. 13. The energy resolutions depend on a number of factors but with careful attention to the detector calibrations noticeably im-

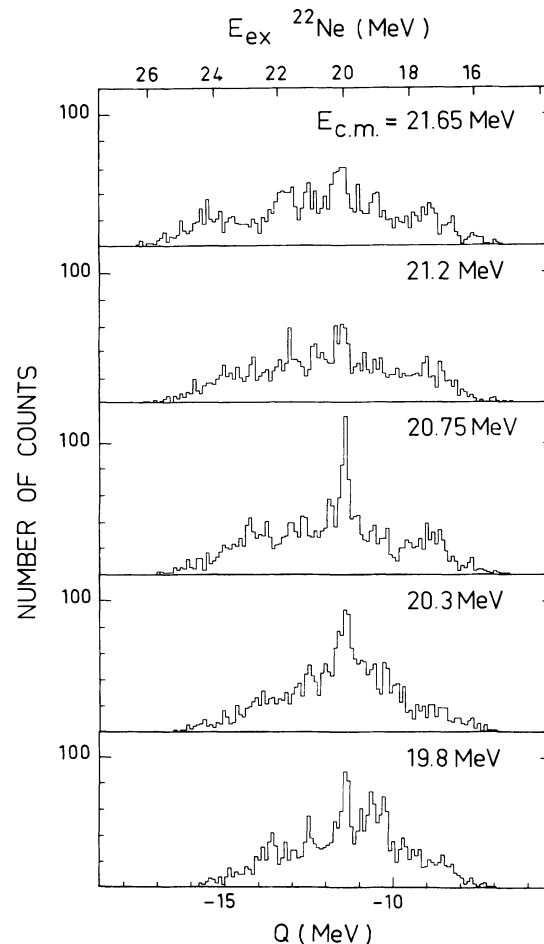


FIG. 14. Spectra of intermediate states of  $^{22}\text{Ne}$  excited by the  $\alpha$ - $\alpha$  chains of the  $^{12}\text{C}(^{14}\text{C}, 2\alpha)^{18}\text{O}^*$  reaction which feed the first  $4^+$  state of  $^{18}\text{O}$ . Results are shown for incident energies ranging over the lower resonance.

proved resolutions are obtained for (1) where only  $\alpha$  particles are detected. Note also the presence of unbound levels and the higher background in Fig. 13(a) due to the less stringent selection conditions in this case.

The two spectra of Fig. 13 correspond to two distinct reaction mechanisms which populate the states differently. For the most part the fusion-evaporation process of the  $2\alpha$  channel should be purely statistical resulting in a preference for feeding the high spin states. This spectrum can then be checked against levels of  $^{18}\text{O}$  compiled by Ajzenberg-Selove [19]. No discrepancies are found for the low-lying levels but at higher excitation energies a reported  $4^+$  state at 9.0 MeV [20] is not seen and further up in the continuum high spin states in the form of three small peaks appear at 10.3, 11.1, and 11.7 MeV where the correspondence with the compilation is uncertain. The energies of the highest two agree well with states at 11.06 and 11.79 MeV which are strongly excited in the  $^{15}\text{N}(^{13}\text{C}, ^{10}\text{B})^{18}\text{O}$  reaction [21] and are proposed to be the  $7^-$  and  $6^-$  states, respectively, formed by coupling a  $p_{1/2}$  hole to the  $13/2^+$  state of  $^{19}\text{F}$ . In the case of the  $^{18}\text{O}^* + ^8\text{Be}$  channel the intensities depend on the spectroscopic factors for  $\alpha$ -particle transfer. As might be expected this spectrum, shown in Fig. 13(b), resembles that for another  $\alpha$ -particle transfer reaction,  $^{14}\text{C}(^7\text{Li}, t)^{18}\text{O}$  [22]. The most prominent peak is a group of unresolved levels of spin no greater than 3.

It is also possible to reconstruct the spectrum of states of  $^{22}\text{Ne}$  which feed the  $^{18}\text{O}$  levels shown in Fig. 13(a). Here an ambiguity arises since the coincident events separate into two branches depending on whether a given detector counts the first or second  $\alpha$  particle in the chain. Being unable to distinguish between the two branches events of only one type will be supposed; the peaks for events of the other branch will be smeared out into the background. An example is shown in Fig. 14 for states in the continuum of  $^{22}\text{Ne}$  which feed the first  $4^+$  state of  $^{18}\text{O}$

at bombarding energies ranging over the lower resonance. In this, as in other examples, states at high excitation energy in  $^{22}\text{Ne}$  are observed to vary rapidly in intensity with energy. The behavior is consistent with a statistical process subject to fluctuations.

## V. CONCLUSION

Considerable structure has been observed in the energy dependence of various channels of the  $^{14}\text{C} + ^{12}\text{C}$  reaction. Much of this structure can be described merely as fluctuations due to the relatively fewer degrees of freedom available to a dinuclear system. However, in three channels we have observed correlated structure in the form of a band of resonances. The spins for two of these resonances were measured and a moment of inertia deduced. The band of resonances corresponds to a system where the  $^{14}\text{C}$  and  $^{12}\text{C}$  orbit each other at a distance where only the tails of the nuclear densities interact. It is therefore assumed that the resonances arise from a molecular configuration held together by the exchange of the outermost nucleons. This dinuclear complex breaks up in three major ways: (1) back into the elastic channel where at large scattering angles the resonant effects stand out and the angular distributions enable firm spin assignments to be made, (2) into the  $^{13}\text{C} + ^{13}\text{C}^*$  (3.85 MeV  $J^\pi = 5/2^+$ ) channel, and (3) into the  $^{12}\text{C} + ^{14}\text{C}^*$  (6.73 MeV  $J^\pi = 3^-$ ) channel. These two reaction channels are closely related as both can result from the promotion of a  $p_{1/2}$  neutron to the  $d_{5/2}$  orbital.

The members of the Frankfurt group, who have done much to advance the idea of molecular orbitals in a two-center shell model, concentrated their efforts for the  $^{26}\text{Mg}$  compound system on the  $^{13}\text{C} + ^{13}\text{C} \rightarrow ^{14}\text{C} + ^{12}\text{C}$  channel [15,16] for which previous data exist [8]. This channel participates little if at all in the resonant behavior. The most interesting phenomena are accessible via the  $^{14}\text{C} + ^{12}\text{C}$  entrance channel.

- 
- [1] R. M. Freeman, F. Haas, and G. Korschinek, *Phys. Lett.* **90B**, 229 (1980).
- [2] F. Haas and Y. Abe, *Phys. Rev. Lett.* **46**, 1667 (1981).
- [3] O. Tanimura, *Z. Phys. A* **319**, 227 (1984).
- [4] D. Konnerth, W. Trombik, K. G. Bernhardt, K. A. Eberhard, R. Singh, A. Strzalkowski, and W. Trautmann, *Nucl. Phys.* **A436**, 538 (1985).
- [5] R. M. Freeman, Z. Basrak, F. Haas, A. Hachem, G. A. Monnehan, and M. Youlal, *Z. Phys. A* **341**, 175 (1992).
- [6] R. J. Ledoux, M. J. Bechara, C. E. Ordonez, H. A. Al-Juwair, and E. R. Cosman, *Phys. Rev. C* **27**, 1103 (1983).
- [7] R. Wieland, A. Gobbi, L. Chua, M. W. Sachs, D. Shapira, R. Stokstad, and D. A. Bromley, *Phys. Rev. C* **8**, 37 (1973).
- [8] S. K. Korotky, K. A. Erb, R. L. Phillips, S. J. Willett, and D. A. Bromley, *Phys. Rev. C* **28**, 168 (1983).
- [9] R. M. Freeman, C. Beck, F. Haas, B. Heusch, H. Bohn, U. Käufl, K. A. Eberhard, H. Puchta, T. Senftleben, and W. Trautmann, *Phys. Rev. C* **24**, 2390 (1981).
- [10] R. M. Freeman, in *Lecture Notes in Physics*, edited by K. A. Eberhard (Springer-Verlag, Berlin, Heidelberg, New York, 1982), Vol. 156, p. 268ff.
- [11] N. Cindro and D. Pocanic, *J. Phys. G* **6**, 359 (1980).
- [12] U. Abbondanno, *Phys. Rev. C* **43**, 1484 (1991).
- [13] D. M. Drake, M. Cates, N. Cindro, D. Pocanic, and E. Holub, *Phys. Lett.* **98B**, 36 (1981).
- [14] W. von Oertzen and H. G. Bohlen, *Phys. Rep.* **19C**, 1 (1975).
- [15] R. Könnecke, W. Greiner, and W. Scheid, *Phys. Rev. Lett.* **51**, 366 (1983).
- [16] A. Thiel, W. Greiner, J. Y. Park, and W. Scheid, *Phys. Rev. C* **36**, 647 (1987).
- [17] R. J. Peterson, H. C. Bhang, J. J. Hamill, and T. G. Masterson, *Nucl. Phys.* **A425**, 469 (1984).
- [18] A. Glaesner, W. Dünnweber, M. Bantel, W. Hering, D. Konnerth, R. Ritzka, W. Trautmann, W. Trombik, and W. Zipper, *Nucl. Phys.* **A509**, 331 (1990).
- [19] F. Ajzenberg-Selove, *Nucl. Phys.* **A475**, 1 (1987).
- [20] H. T. Fortune, L. C. Bland, and W. D. M. Rae, *J. Phys. G* **11**, 1175 (1985).
- [21] W. D. M. Rae, N. S. Godwin, D. Sinclair, H. S. Bradlow, P. S. Fisher, J. D. King, A. A. Pilt, and G. Proudfoot, *Nucl. Phys.* **A319**, 239 (1979).
- [22] M. Gai, M. Ruscev, D. A. Bromley, and J. W. Olness, *Phys. Rev. C* **43**, 2127 (1991).